Simulating HF using FDEM: Effects of pre-existing joints, induced microseismicity and fluid diffusion

Murad S. Abuaisha, David Eaton, Jeffrey Priest, Ron Wong

Simulating HF using FDEM: Effects of pre-existing joints, induced microseismicity and fluid diffusion

Murad AbuAisha[1,2], **David Eaton**[1], **Jeffrey Priest**[2] **and Ron Wong**[2]

[1]*Department of Geoscience, University of Calgary;* [2]*Department of Civil Engineering, University of Calgary, Canada*

murad.abuaisha@ucalgary.ca

Introduction

Hydraulic fracturing (HF) is routinely used in the development of unconventional oil and gas reservoirs. Optimization of this technique requires a detailed understanding of how fractures propagate away from the wellbore especially when existing natural fractures are present. Here we present a numerical study undertaken, using a Finite–Discrete Element Modelling (FDEM) approach to investigate HF growth and induced microseismicity. The first part of the study considers an application of the FDEM called the Y–Geo code that assumes inviscid fluid and accounts for fluid flow only in the fractures, which is convenient for fast fracturing. The Y–Geo code is used here to study the induced microseismicity due to shear slip of critically stressed pre–existing joints. The Y–Geo code is then upgraded to account for fluid leak–off from fractures as well as fluid diffusion in the porous media (the Irazu code). Fluid leak–off and fluid diffusion require long simulation times depending on the permeability of the medium, and are important for simulating Diagnostic Fracture Injection Tests (DFITs). The Irazu code is utilized here to investigate the general response of fluid diffusion and fluid pressure due to changing fluid viscosity as result of changing temperature.

Background

In the FDEM framework, the domain is discretized into elastic triangular elements. The initial elastic deformation of the medium during fluid pressure injection in a borehole is captured by FEM. However, once the medium is fractured, the DEM is used to capture the positions and interaction of fractured blocks.

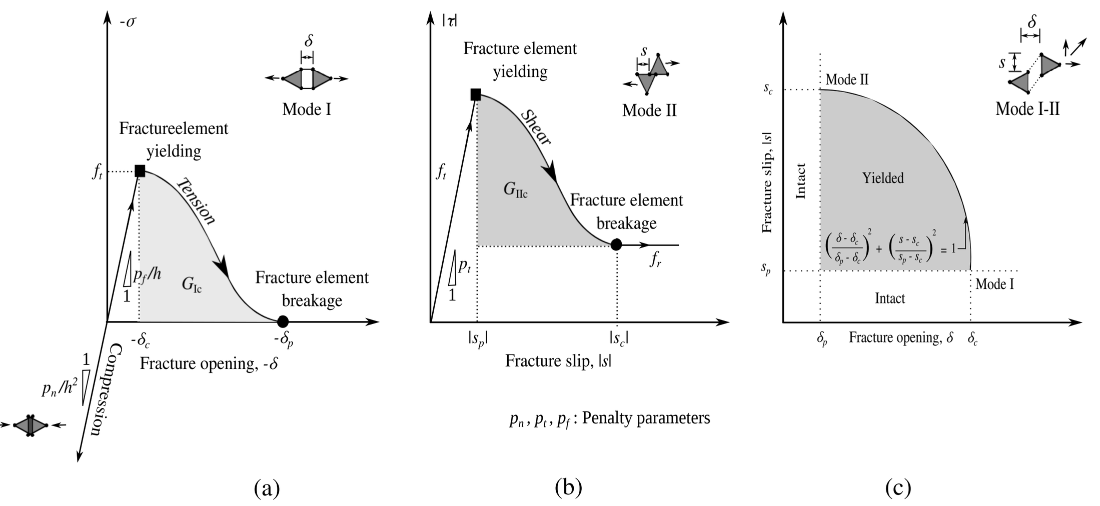

Figure 1: *Penalty coefficients and fracture energies for different modes of fracturing adopted in FDEM [1].*

In FDEM penalty coefficients and fracture energies, related to the cohesive and shear strength of the rock, are used to enable the transition from FEM to DEM behaviour. Figure 1 shows the modelling parameters assigned to different modes of fracturing that occur based on the stress–strain response of the rock. This approach is capable of simulating fracture evolution patterns during HF simulations.

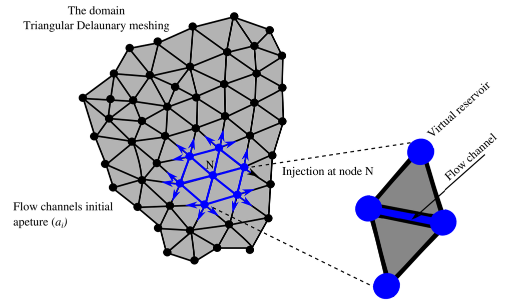

Figure 2: *Conceptual graph that illustrates the implementation of fluid diffusion and leak–off in the FDEM approach.*

Figure 2 illustrates the concept of implementing fluid diffusion and leak–off in the FDEM approach (the Irazu code). The mechanical solver of the Y–Geo code (Fig. 1) is used. Besides, fluid diffusion and fracture leak–off are implemented by considering the existence of flow channels that coincide with the edges of the triangular elements in the initial mesh. The nodes of the triangular elements represent virtual reservoirs where fluid pressure and fluid mass are sequentially calculated. According to the fluid compressibility law, fluid injected at node N will give rise to increased fluid pressure , fluid will then flow to next nodes (virtual reservoirs) through the flow channels due to pressure gradients.

Induced microseismicity due to shear slip (Y-Geo code)

The model adopted to study microseismicity by Y–Geo code is shown in Fig. 3(a). It is a 8m x 8m fractured medium (close to the wellbore), fluid is injected at constant rate 20 l/s.

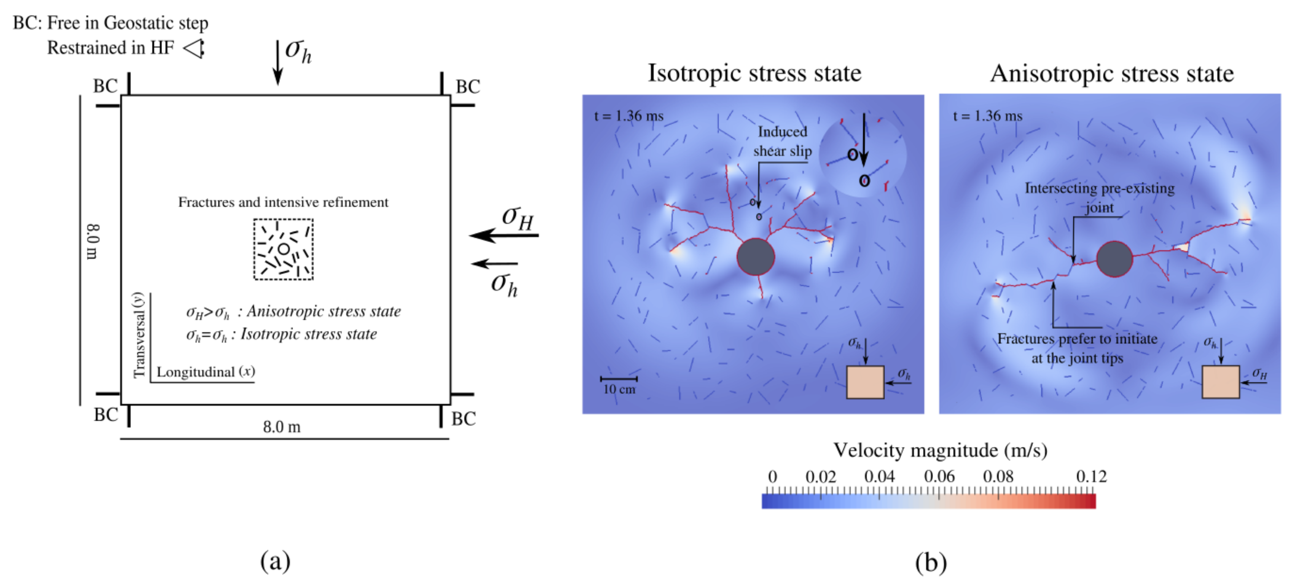

Figure 3: *a) The model of the simulations used in the Y-Geo code. b) Fracture patterns for the cases of isotropic and anisotropic stress states in a heavily fractured rock formation at time of 1.36 ms since injection. The trajectories are plotted in the field of velocity magnitude.*

Figure 3b shows the fracture patterns for two cases of different far–field stresses at time 1.36 ms after initiation of injection. The applied stress state gives rise to different patterns of fluid–driven fractures. Once the growing fracture intersects a pre–existing joint, the joint exploits fluid pressure and leads it to the tips where fracture initiation is accomplished with minimum work. As joints represent planes of weakness, they fracture with less energy and consequently increase the extent to which fluid–driven fractures can reach for the same injected energy.

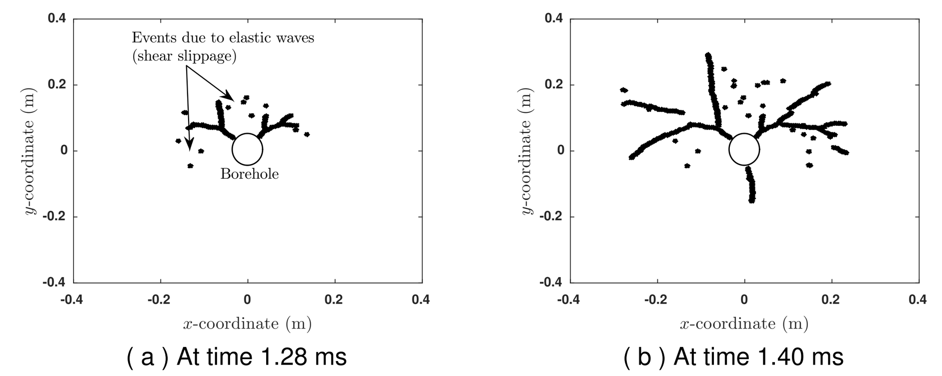

Figure 4: *Microseismic event locations due to fracturing with an isotropic far–field stress state. Microseismic events are following fracture topology except for some scattered locations created by fracturing elastic waves/formation deformation.*

Figure 4 shows the microseismic events locations due to fracturing. It is clear that events are following the patterns of the fluid–driven fractures. However, it is also clear that there are some scattered microseismic incidents that are incited by the deformation of the medium (joint shear slippage) (Fig. 4(a)). Figure 5 shows the magnitudes of the events (as shown in Fig. 4) which range between -4 and -5 as observed in the induced HF microseismicity. It is worthwhile to mention that joint shear slippage can also be caused by fluid diffusion altering critically stressed joints.

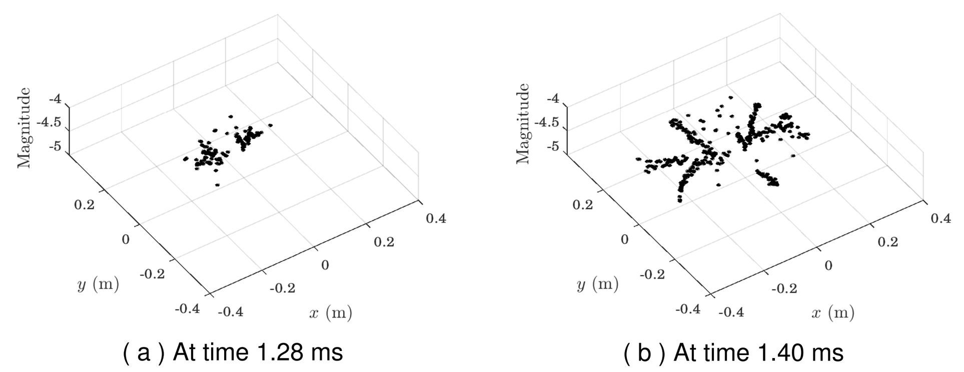

Figure 5: *Magnitudes of the microseismic events presented in Fig. 4. The values are in the range of monitored HF induced microseismicity.*

DFIT simulations: fluid diffusion and leak–off (Irazu code)

The Irazu code utilizes the technique of parallelized calculations, this allows us to use considerably enlarged domains to simulate DFITs with fluid diffusion. Here, our model uses a horizontal wellbore located in 200 m $\times$ 200 m rock formation and drilled in the direction of minimum horizontal stress σ_h, the triangular meshing is also shown (Fig 6). The dimensions of the wellbore are neglected as the research focuses on large scale fracturing and fluid diffusion.

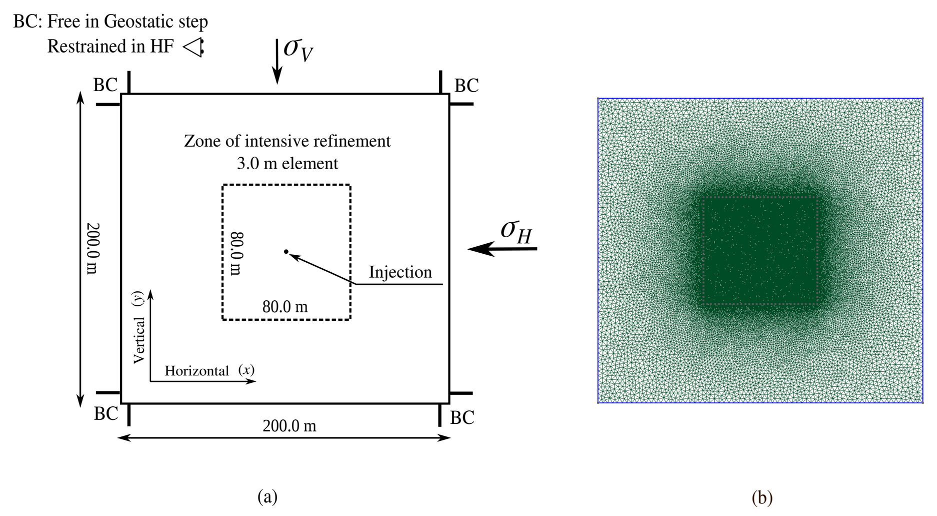

Figure 6: *(a) The geometry and boundary conditions of domain chosen for the HF simulations (Irazu code).*

Fluid is injected following two schemes: 1) at constant flow rate of 0.5 l/s, 2) at stepwise flow rate, where injection is constant (0.5 l/s) for the first 9.1 seconds and then injection is shut down and fluid is left to diffuse/seep across the porous medium.

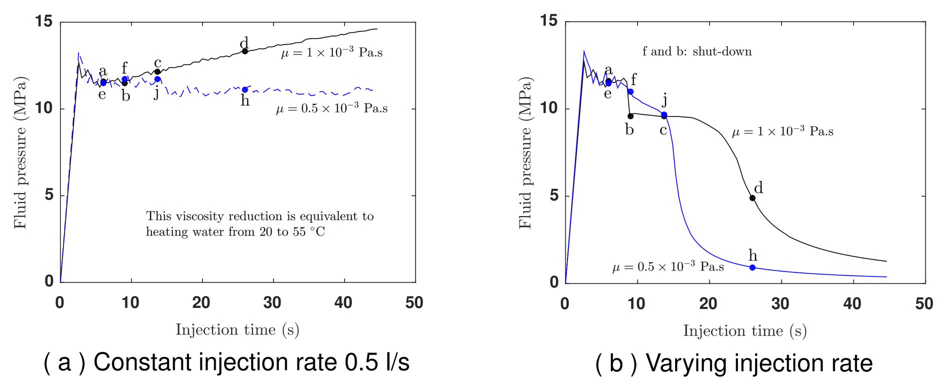

Figure 7: *Net fluid pressure profile due to injection a) at constant rate of 0.5 l/s, b) at constant rate of 0.5 l/s for the first 9.1 s and then shutting down.*

Each of the two schemes is run for two different values of fluid viscosity that correspond to different operating fluid temperatures, i.e. $\mu = 1 \times 10^{-3}$ Pa.s corresponding to $T = 20$ °C and $\mu = 0.5 \times 10^{-3}$ Pa.s corresponding to $T = 55$ °C (for water). Figure 7 shows the injected net fluid pressure profile over a time span of ~45 seconds. Figure 8 shows the contours of the diffused fluid pressure and fracture patterns for the two schemes of injection and for the two possibilities of fluid viscosity. The contours of net fluid pressure and fracture patterns are plotted for different times corresponding to the letters (a to h) in Fig. 7. The letters (a to d) are for the case of viscosity $\mu = 1 \times 10^{-3}$ Pa.s, meanwhile the letters (e to h) are for $\mu = 0.5 \times 10^{-3}$ Pa.s. The letters are picked up such that: 1) a and e correspond to a state in the fracture growing regime (after the fracturing threshold); 2) b and f at the shut down time of 9.1 s; 3) c and j at the state of leak–off (after shut down and before diffusion in the medium); and 4) d and h are during the diffusion process (Fig. 8).

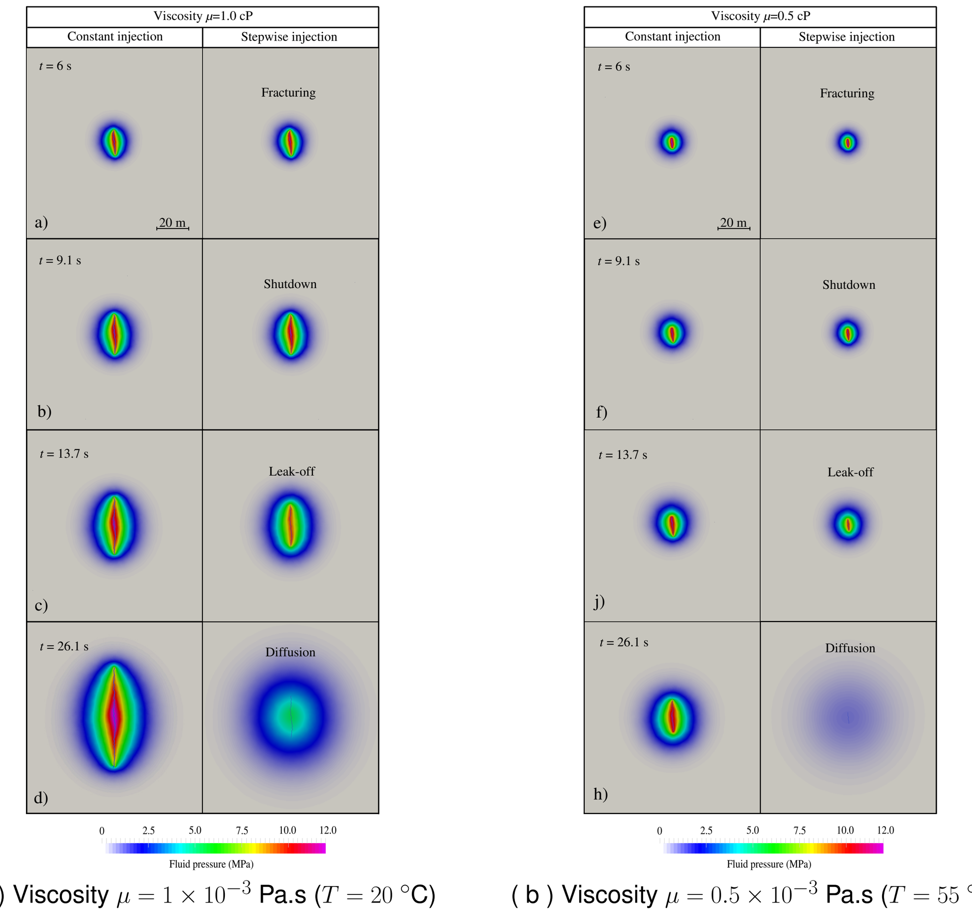

Figure 8: *Fluid driven fracture patterns and diffused fluid pressure contours for the two schemes of injection and for tow different values of fluid viscosity, i.e. $\mu = 1 \times 10^{-3}$ Pa.s corresponding to $T = 20$ °C and $\mu = 0.5 \times 10^{-3}$ Pa.s corresponding to $T = 55$ °C. These contours and fracture patterns are plotted for several injection times which correspond to the letters (a to h) in Fig. 7.*

This part studies the effect of changing fluid viscosity on the entire response of the fluid injection test [2]. It is noticed that for normal values of water viscosity $\mu = 1 \times 10^{-3}$ Pa.s, fluid pressure starts to increase after the breakdown threshold, this is due to the fact that the system becomes less viscosity dominated and more energy is required to grow fractures. However, this result is less evident when fluid is less viscous $\mu = 0.5 \times 10^{-3}$ Pa.s (Fig. 7(a) and Fig. 8(a)). For the case of varying injection flow rate, we can observe that fluid is more diffusive when less viscous, i.e. high temperature values increase the diffusivity of fluid in the rock media (indeed by reducing viscosity) (Fig. 7(b) and Fig. 8(b)).

Conclusions

We have been able to observe that pre–existing joints create a pre–fracturing stress state that affects the patterns of the very initiated fractures and increases the threshold of fracturing. It is also noticed that isolated single pre–existing joints lead to asymmetric fracture growth with tendency for fractures to initiate away from the joints, i.e. possible asymmetric seismicity [3]. However, rock joints increase the extent to which fluid–driven fractures can reach. It is also clear that once a joint is intersected by a fluid–driven fracture, it becomes easier for new fractures to initiate at the joint tips. Induced seismicity study showed that microseismic events due to joint shear slippage can be created by rock deformation only. Such events can go as far as the fluid–driven fractures as long as there are critically stressed joints that might be activated (Fig. 4(b)). We also concluded that changing fluid temperature can considerably change the viscosity of the working fluid and consequently the entire response of fluid diffusion in the porous medium.

References

1. Lisjak A., Mahabadi O. K., Kaifosh P., Vietor T., and Grasselli G. A preliminary evaluation of an enhanced FDEM code as a tool to simulate hydraulic fracturing in jointed rock masses. Rock Engineering and Rock Mechanics: Structures in and on Rock Masses, pages 1427–1432, 2014.
2. Savitski, A. and Detournay, E. Propagation of a penny–shaped fluid–driven fracture in an impermeable rock: Asymptotic solutions. International Journal of Solids and Structures, 39, 6311–6337, 2002.
3. Shapiro S. A. and Dinske C. Fluid–induced seismicity: Pressure diffusion and hydraulic fracturing. Geophysical Prospecting, 57(2):301–310, 2009.

Seismological Society of America (SSA): Annual meeting 2016, 20–22 April, Reno, Nevada, USA. Authors acknowledge the Natural Sciences and Engineering Research Council of Canada (NSERC) and sponsors of the Microseismic Industry Consortium.